



Published in final edited form as:

Bioorg Med Chem Lett. 2017 September 15; 27(18): 4426–4430. doi:10.1016/j.bmcl.2017.08.012.

Design, synthesis, and evaluation of substituted nicotinamide adenine dinucleotide (NAD⁺) synthetase inhibitors as potential antitubercular agents

Xu Wang¹, Yong-Mo Ahn², Adam G. Lentscher¹, Julia S. Lister¹, Robert C. Brothers¹, Malea M. Kneen^{3,a}, Barbara Gerratana⁴, Helena I. Boshoff², and Cynthia S. Dowd^{1,*}

¹Department of Chemistry, George Washington University, Washington DC 20052

²Tuberculosis Research Section, LCID, NIAID/NIH, Bethesda, MD 20892

³Department of Chemistry and Chemical Biology, Indiana University—Purdue University Indianapolis, Indianapolis, IN 46202

⁴Department of Chemistry and Biochemistry, University of Maryland, College Park, MD 20742

Abstract

Nicotinamide adenine dinucleotide (NAD⁺) synthetase catalyzes the last step in NAD⁺ biosynthesis. Depletion of NAD⁺ is bactericidal for both active and dormant *Mycobacterium tuberculosis* (Mtb). By inhibiting NAD⁺ synthetase (NadE) from Mtb, we expect to eliminate NAD⁺ production which will result in cell death in both growing and nonreplicating Mtb. NadE inhibitors have been investigated against various pathogens, but few have been tested against Mtb. Here, we report on the expansion of a series of urea-sulfonamides, previously reported by Brouillette *et al.* Guided by docking studies, substituents on a terminal phenyl ring were varied to understand the structure-activity-relationships of substituents on this position. Compounds were tested as inhibitors of both recombinant Mtb NadE and Mtb whole cells. While the parent compound displayed very weak inhibition against Mtb NadE (IC₅₀ = 1000 μ M), we observed up to a 10-fold enhancement in potency after optimization. Replacement of the 3,4-dichloro group on the phenyl ring of the parent compound with 4-nitro yielded **4f**, the most potent compound of the series with an IC₅₀ value of 90 μ M against Mtb NadE. Our modeling results show that these urea-sulfonamides potentially bind to the intramolecular ammonia tunnel, which transports ammonia from the glutaminase domain to the active site of the enzyme. This hypothesis is supported by data showing that, even when treated with potent inhibitors, NadE catalysis is restored when treated with exogenous ammonia. Most of these compounds also inhibited Mtb cell growth with MIC values of 19–100 μ g/mL. These results improve our understanding of the SAR of the urea-sulfonamides, their mechanism of binding to the enzyme, and of Mtb NadE as a potential antitubercular drug target.

*Corresponding author 800 22nd Street NW, Suite 4000, Washington DC 20052, +1-202-994-8405 (ph), cdowd@gwu.edu.

^aPresent Address: Roche Diagnostics Corporation, Indianapolis, IN 46250

Keywords

Mycobacterium tuberculosis; NadE; antibiotic; antitubercular

Tuberculosis (TB), caused by the bacillus *Mycobacterium tuberculosis* (Mtb), remains one of the world's deadliest infectious diseases.¹⁻³ According to the World Health Organization (WHO) and the Joint United Nations Programme on HIV/AIDS (UNAIDS), 10.4 million people fell ill and 1.8 million died from TB in 2015, which is 0.7 million more than those who died from HIV-related illnesses.^{1, 2} Besides the high prevalence of TB, the large number of new cases of multi-drug resistant (MDR) and extensively-drug resistant (XDR) TB has made the disease a more serious public health concern.² Two of the most important first-line TB drugs (isoniazid, rifampicin) are both ineffective against MDR-TB and XDR-TB, rendering the treatment options very limited.^{4, 5} Thus, there remains a pressing need for novel drugs that shorten TB treatment and are effective against all pathogenic strains.

Nicotinamide adenine dinucleotide (NAD⁺) is a ubiquitous enzyme cofactor, indispensable for reduction-oxidation reactions as well as essential nonredox functions in the cell such as cell longevity, telomere maintenance, Ca²⁺ signaling, DNA repair, and immune response.^{6, 7} NAD⁺ synthetase (NadE) is an essential enzyme that catalyzes the last step in many NAD⁺ *de novo* biosynthesis and NAD⁺ recycling pathways.^{8, 9} In Mtb, NadE transforms nicotinic acid adenine dinucleotide (NaAD⁺) into NAD⁺ via a two-step process with the assistance of ATP and ammonia (Figure 1).⁸⁻¹³ Ammonia is obtained from glutamine hydrolysis in the glutaminase domain of the enzyme.⁸⁻¹³ Inhibition of NadE blocks NAD⁺ biosynthesis and leads to cell death in both growing and nonreplicating Mtb.¹⁴⁻¹⁶ The importance of NAD⁺ encourages the design of NadE inhibitors that may be effective against both active and latent tuberculosis. Moreover, the low sequence identity of 23% between Mtb NadE and the human homolog, as well as the presence of NadE-independent NAD⁺ biosynthesis pathways in humans, increases the attraction of NadE as a drug target for Mtb.^{7, 13, 17, 18}

Despite this promise, few studies explore NadE inhibitors as antitubercular agents. Velu *et al.* reported a series of tethered dimers as inhibitors of *B. subtilis* NadE and several Gram-positive organisms.^{16, 19} One of the most potent *B. subtilis* NadE inhibitors from this work (Figure 2A) yielded an IC₅₀ (concentration resulting in 50% enzyme inhibition) value of 10 μ M against *B. subtilis* NadE and an MIC (minimum inhibitory concentration) of 1.5 μ M against *B. subtilis*.^{16, 19} Boshoff *et al.* tested several of these tethered dimers against Mtb NadE and Mtb cellular growth.¹⁴ The compounds, however, showed only modest activity. The most potent Mtb NadE inhibitor (Figure 2B) gave an IC₅₀ of 21.8 μ M against Mtb NadE and an Mtb MIC of 20 μ M.¹⁴

A significant number of compounds as inhibitors of NadE have been synthesized by the Brouillette group.^{20, 21} Using a high-throughput assay, they discovered compound **5824**, which showed strong inhibition of *B. anthracis* NadE (IC₅₀ = 6.4 μ M, Figure 2).²⁰ According to their modeling results using the *B. subtilis* homolog, the group predicted that **5824** bound to the NaAD⁺ subsite of NadE.²⁰ The group next reported a series of the reverse sulfonamide analogs of **5824** that were tested against *B. anthracis* NadE, *B. anthracis*

NaMNAT, and *B. anthracis* Sterne. One of their best inhibitors (Figure 2C) displayed a *B. anthracis* NadE IC₅₀ of 15.3 μ M but did not kill *B. anthracis* cells.²¹

In order to evaluate compounds that are active against *Bacillus* NadE as potential Mtb NadE inhibitors, the similarity between *Bacillus* and Mtb homologs was explored. Mtb NadE is glutamine dependent and has a glutaminase domain that transports ammonia to the synthetase domain via an ammonia tunnel.¹¹ Interestingly, NadE from *B. subtilis* or *B. anthracis* depends on exogenous ammonia and does not possess a glutaminase domain or an ammonia tunnel.^{22, 23} Thus, the amino acid sequences of NadE from *B. subtilis*, *B. anthracis*, and only the C-terminal domain of Mtb NadE (*i.e.*, the Mtb NadE synthetase domain that is homologous to the *Bacillus* NadE enzymes) were aligned. The sequence identity among these enzymes was calculated based on this alignment using MUSCLE^{24, 25} (Table 1). While the two *Bacillus* NadEs share 88.6% sequence identity, the Mtb NadE C-terminal domain shares 36.6% sequence identity to the *Bacillus subtilis* NadE and 34.4% sequence identity to the *Bacillus anthracis* NadE. We expected high conservation of the active site residues between species, which encourages the design of Mtb NadE inhibitors based on the *Bacillus* inhibitor structures. Therefore, we chose compound **5824** (3-{4-[(3,4 dichlorophenyl)sulfamoyl]phenyl}-1-(4-nitrophenyl)urea, Figure 2) as the parent structure for the current work.

A virtual library of 118 urea-sulfonamide analogs was made. Half of the compounds were sulfonamides, retaining the configuration of parent compound **5824**, while half were the ‘reversed sulfonamide’, corresponding to the opposite configuration. Compounds varied structurally only at ring A, where a variety of substituents were appended. Substituents were selected based on the Topliss approach toward aromatic systems²⁶ as well as commercially available anilines. Compounds were docked into the crystal structure of Mtb NadE¹³ (PDB id: 3DLA) using the Glide tool in Schrodinger, suite 2010²⁷. The 100 top-scoring analogs are shown in Table S1 (more negative Glide scores predicting improved binding affinities). Interestingly, the putative binding site of many analogs was predicted to involve the intramolecular ammonia tunnel¹¹ that transports ammonia from the glutaminase domain to the synthetase domain (Table S2). For example, compound **41** (R = 4-H) formed hydrogen bonds with GLY-366 and LEU-399 (Figure 3A), and ring A rested in a hydrophobic pocket, the entrance to the tunnel (Figure 3B). Based on these modeling results and synthetic feasibility, a series of analogs was selected for synthesis (Figure 4). These compounds could shed light on the influence of ring A structural changes on Mtb NadE inhibition and antibacterial activity.

To prepare the desired compounds, a simple synthetic route was designed (Scheme 1). Substituted anilines *1a-l* were combined with 4-acetamidobenzenesulfonyl chloride to obtain compounds *2a-l* generally in high yield unless a second recrystallization in ethanol was needed. The deacetylated products (*3a-l*) were obtained after acid hydrolysis and were purified either by silica column chromatography or recrystallization. The intermediates *3a-l* were then combined with 4-nitrophenylisocyanate to yield final compounds *4a-l*. Due to production of a sticky side product (likely a urea), purification of some final compounds proved challenging. Such reactions were purified by silica column chromatography and then

by recrystallization from acetone to achieve high purity but with substantially reduced yields²⁸⁻³¹

Compounds were evaluated for inhibition of Mtb NadE measuring their effect on pyrophosphate (PPi) production using the EnzChek Pyrophosphate Assay (ThermoFisher, Waltham, MA). Briefly, PPi formation is coupled to the production of 2-amino-6-mercapto-7-methylpurine at 360 nm. The IC₅₀ values are shown in Table 2. The synthesized urea-sulfonamide compounds show a 10-fold range of activity against Mtb NadE. Parent compound *4i* (5824) shows poor inhibition of Mtb NadE (IC₅₀ = 1000 ± 300 μM), contrary to its more potent inhibition of *B. anthracis* NadE (IC₅₀ = 6.4 μM).²¹ This difference in efficacy is likely due to structural differences between the two homologs (as noted above). Our modeling results show that the binding site of this series of compounds may involve the intramolecular ammonia tunnel of the Mtb NadE. This tunnel is absent in *B. subtilis* and *B. anthracis*. Thus, compound *4i* likely binds to an alternate site in the *Bacillus* homologs compared with Mtb NadE.

The new analogs show improved Mtb NadE inhibition relative to the parent compound with most IC₅₀ values roughly 5-10-fold better than *4i*. The most potent Mtb NadE inhibitor of the series is *4f* (4-NO₂) with an IC₅₀ value of 90 μM. Comparing unsubstituted analog *4l* with other analogs in the series, halogen-substituents are generally not beneficial in terms of Mtb NadE inhibition as compounds *4e*, *4j*, and *4k* were among the least potent of the series. The remaining analogs, *4a-d* and *4f-h* have similar activities compared to unsubstituted compound *4l* and yield a bland structure-activity-relationship profile between these substituents and Mtb NadE inhibition.

To further investigate the binding mechanism of this series of compounds, an ammonia-dependent Mtb NadE inhibition assay^{12, 32} was performed on the most potent compounds *4d*, *4f*, *4h* and *4l*. In this assay, exogenous ammonia is used as the ammonia source for the NadE reaction, as opposed to the ammonia synthesized by the glutaminase domain of the enzyme. As shown in Table 2, these compounds lose inhibition (IC₅₀ > 200 μM) against Mtb NadE when exogenous ammonia is supplied, and enzymatic activity is restored. This supports our hypothesis that these compounds bind to the intramolecular ammonia tunnel suggested from the modeling study, as well as offering an explanation of the activity difference observed for compound *4i* against *B. anthracis* NadE versus Mtb NadE.

The urea-sulfonamides were also tested for the inhibition of Mtb cellular growth in both rich media (7H9) and minimal media (GAST-Fe).³³⁻³⁶ The antitubercular activities of these compounds are shown in Table 2. All compounds inhibit Mtb growth to a moderate extent with MIC values of 19-100 μg/mL (7H9). The most potent compound is *4e* (4-F) with an MIC value of 19 μg/mL (7H9). Again, the structure-activity relationship of the series is flat, indicating this portion of the urea-sulfonamides does not impact antitubercular activities to a great extent.

There remains an urgent need for antitubercular drugs that are highly active and work through new modes of actions. This work builds on the novel design of three-ring urea-sulfonamides as NadE inhibitors. The parent compound *4i*, shows very different potency

against Mtb and *B. anthracis* NadE homologs, perhaps due to structural differences between the two enzymes. This is supported by our preliminary modeling studies, showing that the binding sites of these compounds may overlap with the ammonia tunnel in Mtb NadE rather than the NaAD⁺ subsite in *B. anthracis* NadE²⁰, as suggested earlier. This hypothesis is reinforced by the loss of activities for the active Mtb NadE inhibitors when treated with exogenous ammonia instead of that from glutamine. This point of difference may be used to design selective inhibitors targeting Mtb NadE over other homologs. While most of the analogs display a 5-10-fold improvement against Mtb NadE over the parent compound, all of the compounds show moderate activity against Mtb whole cell growth. Structural optimization of these compounds is needed, not only to improve activity against both Mtb NadE and Mtb, but also to increase solubility which was noticeably poor in various organic solvents and water. Such compounds would aid in further validating NadE as an effective target for Mtb and other bacterial pathogens.

Supplementary Material

Refer to Web version on PubMed Central for supplementary material.

Acknowledgments

We thank Nigel Richards (Cardiff University) for helpful discussions throughout this project. This work was generously supported by the George Washington University (GWU) Department of Chemistry, the GWU University Facilitating Fund, the American Chemical Society (PRF to BG), the University of Maryland College Park Department of Chemistry and Biochemistry, and the Division of Intramural Research, NIAID, NIH.

References and Notes

1. Global HIV Statistics, The Joint United Nations Programme on HIV/AIDS. http://www.unaids.org/sites/default/files/media_asset/UNAIDS_FactSheet_en.pdf
2. Global Tuberculosis Report 2016, World Health Organization. http://www.who.int/tb/publications/global_report/en/
3. The world's deadliest disease just got deadlier, TB Europe Coalition. <http://www.tbcoalition.eu/2016/10/14/the-worlds-deadliest-disease-just-got-deadlier/>
4. TB Elimination Extensively Drug-Resistant Tuberculosis (XDR-TB), Centers for Disease Control and Prevention. <https://www.cdc.gov/tb/publications/factsheets/drtb/mdrtb.pdf>
5. TB Elimination Extensively Drug-Resistant Tuberculosis (XDR-TB), Centers for Disease Control and Prevention. <https://www.cdc.gov/tb/publications/factsheets/drtb/xdrtb.pdf>
6. Belenky P; Bogan KL; Brenner C NAD⁺ metabolism in health and disease. Trends in Biochemical Sciences 32, 12–19. [PubMed: 17161604]
7. Bi J; Wang H; Xie J Comparative genomics of NAD(P) biosynthesis and novel antibiotic drug targets. Journal of Cellular Physiology 2011, 226, 331–340. [PubMed: 20857400]
8. Spencer RL; Preiss J Biosynthesis of Diphosphopyridine Nucleotide: THE PURIFICATION AND THE PROPERTIES OF DIPHOSPHOPYRIDINE NUCLEOTIDE SYNTHETASE FROM ESCHERICHIA COLI B. Journal of Biological Chemistry 1967, 242, 385–392. [PubMed: 4290215]
9. Raushel FM; Thoden JB; Holden HM The Amidotransferase Family of Enzymes: Molecular Machines for the Production and Delivery of Ammonia. Biochemistry 1999, 38, 7891–7899. [PubMed: 10387030]
10. Resto M; Yaffe J; Gerratana B An ancestral glutamine-dependent NAD⁺ synthetase revealed by poor kinetic synergism. Biochimica et Biophysica Acta (BBA) - Proteins and Proteomics 2009, 1794, 1648–1653. [PubMed: 19647806]

11. Chuenchor W; Doukov Tzanko I; Resto M; Chang A; Gerratana B Regulation of the intersubunit ammonia tunnel in Mycobacterium tuberculosis glutamine-dependent NAD⁺ synthetase. *Biochemical Journal* 2012, 443, 417–426. [PubMed: 22280445]
12. De Ingeniis J; Kazanov MD; Shatalin K; Gelfand MS; Osterman AL; Sorci L Glutamine versus Ammonia Utilization in the NAD Synthetase Family. *PLOS ONE* 2012, 7, e39115. [PubMed: 22720044]
13. LaRonde-LeBlanc N; Resto M; Gerratana B Regulation of active site coupling in glutamine-dependent NAD⁺ synthetase. *Nat Struct Mol Biol* 2009, 16, 421–429. [PubMed: 19270703]
14. Boshoff HIM; Xu X; Tahlan K; Dowd CS; Pethe K; Camacho LR; Park T-H; Yun C-S; Schnappinger D; Ehrst S; Williams KJ; Barry CE Biosynthesis and Recycling of Nicotinamide Cofactors in Mycobacterium tuberculosis: AN ESSENTIAL ROLE FOR NAD IN NONREPLICATING BACILLI. *Journal of Biological Chemistry* 2008, 283, 19329–19341. [PubMed: 18490451]
15. Kim J-H; O'Brien KM; Sharma R; Boshoff HIM; Rehren G; Chakraborty S; Wallach JB; Monteleone M; Wilson DJ; Aldrich CC; Barry CE; Rhee KY; Ehrst S; Schnappinger D A genetic strategy to identify targets for the development of drugs that prevent bacterial persistence. *Proceedings of the National Academy of Sciences* 2013, 110, 19095–19100.
16. Velu SE; Cristofoli WA; Garcia GJ; Brouillette CG; Pierson MC; Luan C-H; DeLucas LJ; Brouillette WJ Tethered Dimers as NAD Synthetase Inhibitors with Antibacterial Activity. *Journal of Medicinal Chemistry* 2003, 46, 3371–3381. [PubMed: 12852767]
17. Mori V; Amici A; Mazzola F; Di Stefano M; Conforti L; Magni G; Ruggieri S; Raffaelli N; Orsomando G Metabolic Profiling of Alternative NAD Biosynthetic Routes in Mouse Tissues. *PLOS ONE* 2014, 9, e113939. [PubMed: 25423279]
18. Revollo JR; Grimm AA; Imai S-i. The NAD Biosynthesis Pathway Mediated by Nicotinamide Phosphoribosyltransferase Regulates Sir2 Activity in Mammalian Cells. *Journal of Biological Chemistry* 2004, 279, 50754–50763. [PubMed: 15381699]
19. Velu SE; Mou L; Luan C-H; Yang ZW; DeLucas LJ; Brouillette CG; Brouillette WJ Antibacterial Nicotinamide Adenine Dinucleotide Synthetase Inhibitors: Amide- and Ether-Linked Tethered Dimers with α -Amino Acid End Groups. *Journal of Medicinal Chemistry* 2007, 50, 2612–2621. [PubMed: 17489580]
20. Moro WB; Yang Z; Kane TA; Brouillette CG; Brouillette WJ Virtual screening to identify lead inhibitors for bacterial NAD synthetase (NADs). *Bioorganic & Medicinal Chemistry Letters* 2009, 19, 2001–2005. [PubMed: 19249205]
21. Moro WB; Yang Z; Kane TA; Zhou Q; Harville S; Brouillette CG; Brouillette WJ SAR Studies for a New Class of Antibacterial NAD Biosynthesis Inhibitors. *Journal of Combinatorial Chemistry* 2009, 11, 617–625. [PubMed: 19408950]
22. Devedjiev Y; Symersky J; Singh R; Jedrzejewski M; Brouillette C; Brouillette W; Muccio D; Chattopadhyay D; DeLucas L Stabilization of active-site loops in NH₃-dependent NAD⁺ synthetase from *Bacillus subtilis*. *Acta Crystallographica Section D* 2001, 57, 806–812.
23. McDonald HM; Pruett PS; Deivanayagam C; Protasevich II; Carson WM; DeLucas LJ; Brouillette WJ; Brouillette CG Structural adaptation of an interacting non-native C-terminal helical extension revealed in the crystal structure of NAD⁺ synthetase from *Bacillus anthracis*. *Acta Crystallographica Section D* 2007, 63, 891–905.
24. Edgar RC MUSCLE: multiple sequence alignment with high accuracy and high throughput. *Nucleic Acids Research* 2004, 32, 1792–1797. [PubMed: 15034147]
25. Edgar RC MUSCLE: a multiple sequence alignment method with reduced time and space complexity. *BMC Bioinformatics* 2004, 5, 113. [PubMed: 15318951]
26. Topliss JG Utilization of operational schemes for analog synthesis in drug design. *Journal of Medicinal Chemistry* 1972, 15, 1006–1011. [PubMed: 5069767]
27. Friesner RA; Murphy RB; Repasky MP; Frye LL; Greenwood JR; Halgren TA; Sanschagrin PC; Mainz DT Extra Precision Glide: Docking and Scoring Incorporating a Model of Hydrophobic Enclosure for Protein-Ligand Complexes. *Journal of Medicinal Chemistry* 2006, 49, 6177–6196. [PubMed: 17034125]

28. Compound 4e. To a solution of the 3e (1 eq) in anhydrous THF (30 mL/mmol) was added 4-nitrophenylisocyanate (1 eq). The reaction mixture was stirred at room temperature overnight, concentrated. Silica cake was prepared in acetone and chromatographic separation on silica gel (EtOAc/CH₂Cl₂ = 1/30 to 1/5) gave the crude solids which were further recrystallized in acetone to give the expected compound as white solids. Yield: 14%. ¹H NMR (acetone-d₆, 400 MHz), δ (ppm): 6.99-7.07 (m, 2H), 7.20-7.25 (m, 2H), 7.63-7.71 (m, 4H), 7.76-7.81 (m, 2H), 8.17-8.23 (m, 2H), 8.74 (s, 1H), 8.89 (s, 1H), 8.93 (s, 1H). ¹³C NMR (acetone-d₆, 100 MHz), δ (ppm): 116.53, 116.76, 119.02, 119.14, 124.57, 124.65, 125.84, 129.36, 133.97, 135.20, 135.23, 143.31, 144.52, 146.83, 152.62, 159.79, 162.19. LC/MS (ESI) m/z: 431 (M+1), 861 (2M+1).
29. Compound 4f. To a solution of the 3f (1 eq) in anhydrous THF (30 mL/mmol) was added 4-nitrophenylisocyanate (1 eq). The reaction mixture was stirred at room temperature overnight, concentrated. Silica cake was prepared in acetone and chromatographic separation on silica gel (EtOAc/CH₂Cl₂ = 1/30 to 1/5) gave the crude solids which were further recrystallized in acetone to give the expected compound as yellow solids. Yield: 7%. ¹H NMR (acetone-d₆, 400 MHz), δ (ppm): 7.48-7.54 (m, 2H), 7.74-7.85 (m, 4H), 7.88-7.94 (m, 2H), 8.18-8.27 (m, 4H), 8.81 (s, 1H), 8.94 (s, 1H), 9.79 (s, 1H). ¹³C NMR (acetone-d₆, 100 MHz), δ (ppm): 118.95, 119.27, 119.31, 125.72, 126.00, 129.40, 133.44, 143.26, 144.99, 145.25, 146.60, 150.95, 152.43. LC/MS (ESI) m/z: 458 (M+1), 915 (2M+1).
30. Compound 4h. To a solution of the 3h (1 eq) in anhydrous THF (30 mL/mmol) was added 4-nitrophenylisocyanate (1 eq). The reaction mixture was stirred at room temperature overnight, concentrated. Silica cake was prepared in acetone and chromatographic separation on silica gel (EtOAc/CH₂Cl₂ = 1/30 to 1/5) gave the crude solids which were further recrystallized in acetone to give the expected compound as light yellow solids. Yield: 13%. ¹H NMR (acetone-d₆, 400 MHz), δ (ppm): 7.26-7.33 (m, 1H), 7.38-7.42 (m, 2H), 7.43-7.48 (m, 1H), 7.58-7.63 (m, 2H), 7.65-7.70 (m, 4H), 8.06-8.13 (m, 2H), 8.60 (s, 1H), 8.76 (s, 1H), 9.19 (s, 1H). ¹³C NMR (acetone-d₆, 100 MHz), δ (ppm): 117.33, 118.92, 119.18, 121.49, 124.49, 125.71, 129.28, 131.19, 133.59, 139.91, 143.22, 144.70, 146.62, 152.42. LC/MS (ESI) m/z: 481 (M+1).
31. Compound 4l. To a solution of the 3l (1 eq) in anhydrous THF (30 mL/mmol) was added 4-nitrophenylisocyanate (1 eq). The reaction mixture was stirred at room temperature overnight, concentrated. Silica cake was prepared in acetone and chromatographic separation on silica gel (EtOAc/CH₂Cl₂ = 1/30 to 1/5) gave the crude solids which were further recrystallized in acetone to give the expected compound as white solids. Yield: 8%. ¹H NMR (acetone-d₆, 400 MHz), δ (ppm): 7.04-7.08 (m, 1H), 7.20-7.29 (m, 4H), 7.64-7.82 (m, 6H), 8.18-8.23 (m, 2H), 8.66 (s, 1H), 8.85 (s, 1H), 8.87 (s, 1H). ¹³C NMR (acetone-d₆, 100 MHz), δ (ppm): 119.00, 119.08, 119.14, 119.22, 121.78, 125.39, 125.90, 129.41, 130.14, 134.50, 139.18, 144.49, 152.57. LC/MS (ESI) m/z: 413 (M+1), 825 (2M+1).
32. Boehlein SK; Richards NG; Schuster SM Glutamine-dependent nitrogen transfer in *Escherichia coli* asparagine synthetase B. Searching for the catalytic triad. *Journal of Biological Chemistry* 1994, 269, 7450–7457. [PubMed: 7907328]
33. Kim P; Zhang L; Manjunatha UH; Singh R; Patel S; Jiricek J; Keller TH; Boshoff HI; Barry CE; Dowd CS Structure–Activity Relationships of Antitubercular Nitroimidazoles. 1. Structural Features Associated with Aerobic and Anaerobic Activities of 4- and 5-Nitroimidazoles. *Journal of Medicinal Chemistry* 2009, 52, 1317–1328. [PubMed: 19209889]
34. San Jose G; Jackson ER; Uh E; Johnny C; Haymond A; Lundberg L; Pinkham C; Kehm-Hall K; Boshoff HI; Couch RD; Dowd CS Design of potential bisubstrate inhibitors against *Mycobacterium tuberculosis* (Mtb) 1-deoxy-d-xylulose 5-phosphate reductoisomerase (Dxr)-evidence of a novel binding mode. *MedChemComm* 2013, 4, 1099–1104. [PubMed: 23914289]
35. Yendapally R; Hurdle JG; Carson EI; Lee RB; Lee RE N-Substituted 3-Acetyltetramic Acid Derivatives as Antibacterial Agents. *Journal of Medicinal Chemistry* 2008, 51, 1487–1491. [PubMed: 18281930]
36. San Jose G; Jackson ER; Haymond A; Johnny C; Edwards RL; Wang X; Brothers RC; Edelstein EK; Odom AR; Boshoff HI; Couch RD; Dowd CS Structure-Activity Relationships of the MEPicides: N-Acyl and O-Linked Analogs of FR900098 as Inhibitors of Dxr from *Mycobacterium tuberculosis* and *Yersinia pestis*. *ACS Infectious Diseases* 2016, 2, 923–935. [PubMed: 27676224]

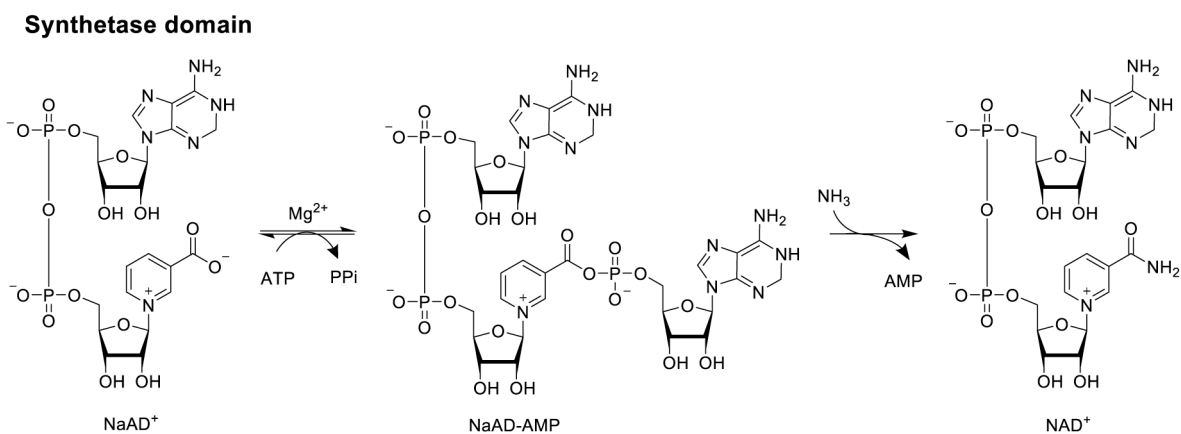
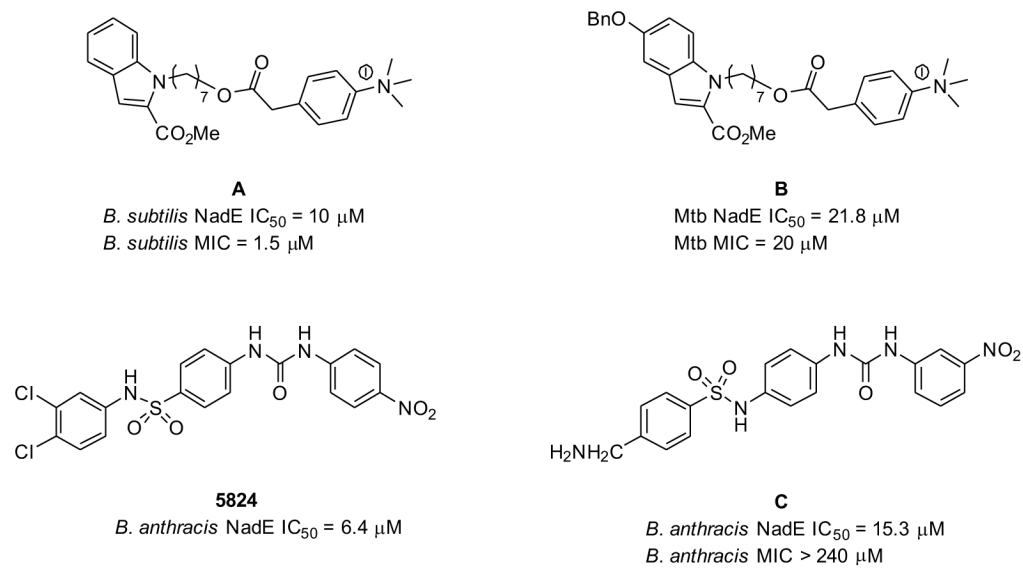


Figure 1.
Two-step reaction catalyzed by NAD⁺ synthetase.

**Figure 2.**

Structures and bioactivities of known NadE inhibitors.14, 16, 19, 20

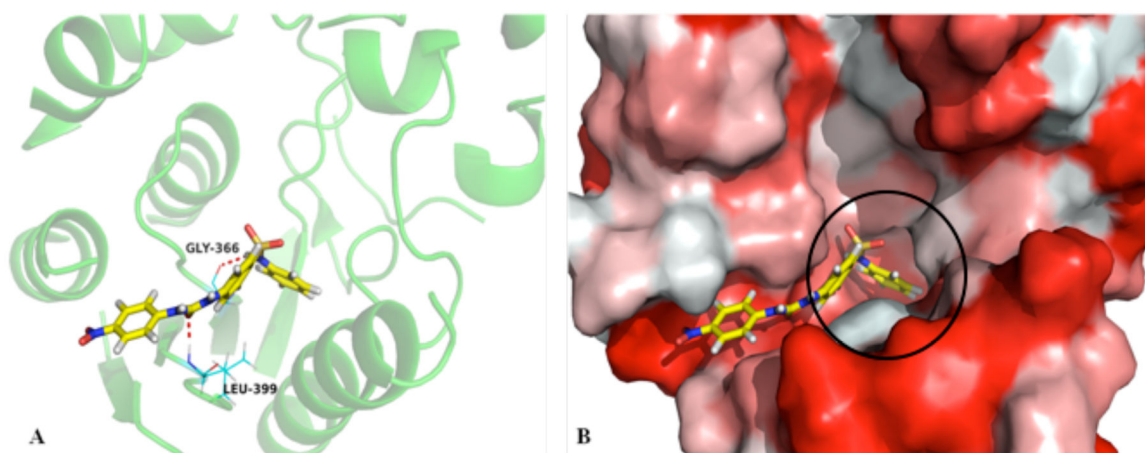
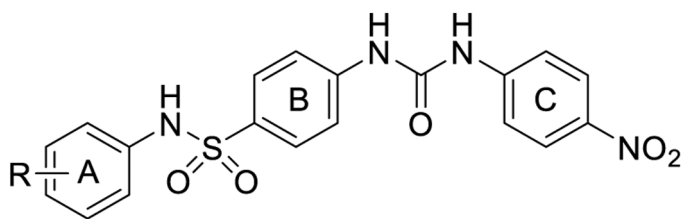


Figure 3.

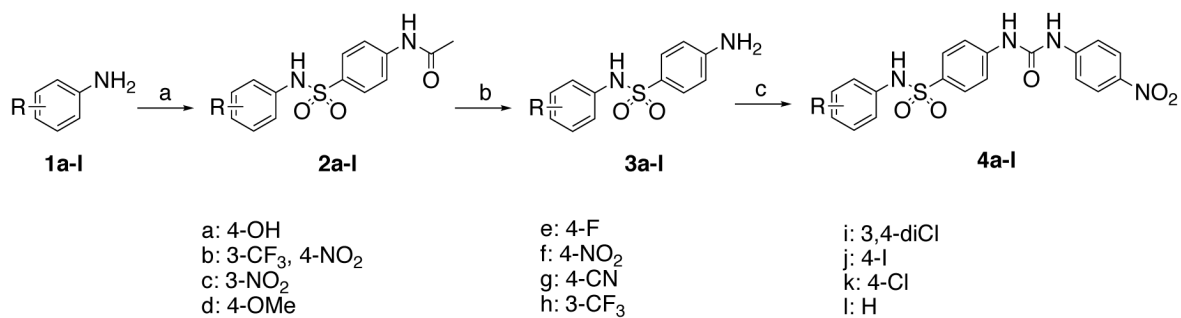
Compound **41** (R = 4-H) docked into Mtb NadE (PDB: 3DLA). (A) The green ribbon represents NadE. The ligand and selected protein residues are colored by atom type, and hydrogen bonding is represented by dashed red lines. (B) Using the same NadE orientation, the surface of the enzyme is colored to show the degree of hydrophobicity (darker red indicates more hydrophobic character). Ring A (circled) is shown going into the ammonia tunnel at its entrance.



R = 4-H; 4-OH; 4-OMe; 4-F; 4-Cl; 4-I; 3,4-diCl (**5824**);
3-CF₃; 3-NO₂; 4-NO₂; 4-CN; 3-CF₃, 4-NO₂.

Figure 4.

Structure of parent compound **5824** and the analogs prepared in this work.

**Scheme 1.**

Reagents and conditions: a) pyridine, 4-AcNHPhSO₂Cl; b) HCl; c) 4-NO₂PhNCO

Table 1.Sequence identity between NadE synthetase homologs from Mtb, *B. subtilis* and *B. anthracis*

Sequence Identity (%)	<i>B. subtilis</i> NadE	<i>B. anthracis</i> NadE	Mtb NadE (C-term Synthetase domain)
Mtb NadE C-term Synthetase domain	36.6		
<i>B. subtilis</i> NadE		88.6	
<i>B. anthracis</i> NadE			34.4

Table 2.

Mtb NadE inhibition and growth inhibition of urea-sulfonamide analogs

Compound	R	Mtb NadE IC ₅₀ (μM) Gln-dependent	Mtb NadE IC ₅₀ (μM) NH ₃ -dependent	Mtb MIC (μg/mL) 7H9	Mtb MIC (μg/mL) GAST-Fe
4a	4-OH	160 ± 20		37	50
4b	3-CF ₃ , 4-NO ₂	190 ± 10		100	50
4c	3-NO ₂	170 ± 20		25	12.5
4d	4-OMe	130 ± 10	>200	25	50
4e	4-F	170 ± 20		19	25
4f	4-NO ₂	90 ± 5	>200	37	25
4g	4-CN	190 ± 10		37	37
4h	3-CF ₃	130 ± 20	>200	37	50
4i	3,4-diCl (5824 ²⁰)	1000 ± 300		25	50
4j	4-I	370 ± 10		37	50
4k	4-Cl	520 ± 100		25	37
4l	H	125 ± 5	>200	75	12.5
INH				0.05	0.03

Mtb = *Mycobacterium tuberculosis*; IC₅₀ = inhibitor concentration resulting in 50% enzyme inhibition; MIC = minimum inhibitory concentration; 7H9 = rich media; GAST = minimal media; INH= isoniazid